Numerical Investigation into Ship Stability Failure Events in Quartering Seas Based on Time Domain Weakly Nonlinear Unified Model

Liwei Yu, Ning Ma* and Xiechong Gu
State Key Laboratory of Ocean Engineering, Shanghai Jiao Tong University, China

Abstract: A 6-DOF weakly nonlinear unified model considering sea-keeping motion at low frequency, maneuvering motion and rudder propeller hydrodynamics is developed for the numerical analysis of ship stability failure events in quartering seas. In the model, the maneuvering and seakeeping models are solved in different time scale and combined together based on the Unified theory. The model is applied to the ITTC ship A2 fishing vessel. Motions in regular astern waves with possible stability failure are simulated and compared with experiment results obtained from the literature. Results show that the weakly nonlinear model is capable of reproducing stability failure events like steady surf-riding, capsizing due to broaching and capsizing without broaching. However the quantitative agreement between simulation and experiment results of the ITTC ship A2 are not good enough at the moment. The present model seems to overestimate the possibility of stability failure somewhat and the reasons are discussed consequently

Key words: Weakly nonlinearity, unified theory, stability failure mode, surf-riding, broaching

1. Introduction

Ship sailing in severe following/quartering seas may suffer from loss of control and stability. Such phenomena like surf-riding and broaching have been recognized as the causes of ship capsizing in high astern seas. Unlike normal periodic ship motion, surf-riding is non-periodic and occurs when ship is overtaken by wave astern and forced to sail with wave celerity. Broaching happens when ship heading changes suddenly and lose its course-keeping ability. Both phenomena are strongly nonlinear which often happens on small fishing vessels and can cause ship dynamic stability problems, even capsizing [1].

Theoretical study on surf-riding and broaching dates back to 1950s. Pioneering researches on surf-riding and broaching in following seas are done based on uncoupled surge equation with nonlinear wave induced surging force[2],[3]. Theoretical solutions in regular and irregular waves show the occurrence of surf-riding in a certain range of propeller thrust. Due to difficulties in getting an analytical solution for the nonlinear problem, steady state and bifurcation analysis in nonlinear dynamics are applied. Umeda and Kohyama [4], Umeda [5] conducted phase plane analysis on the nonlinear surge equation with different initial conditions on basis of the works done by a Russian researcher [6]. Lately, an analytical formula for prediction of surf-riding threshold is proposed based on the Melnikov's method [7].Furthermore, the nonlinear steady state analysis are applied on a surge-sway-yaw-roll model, recently a 6-DOF model [8-11]. Boundaries between periodic motion, surf-riding, broaching and capsizing are discussed. These analytic and nonlinear dynamic approaches show advantages in analyzing the dependence on initial conditions and determining the critical conditions for surf-riding and broaching.

Model experiments is useful for understanding the physical mechanism of ship surf-riding and broaching

in following/quartering seas. Moreover the experiment results can be used for the validation of numerical models. Umeda et al. [12] conduct model experiment to assess the stability of two fishing vessels in quartering sea. Broaching, broaching without capsizing, nearly broaching and capsizing due to bow diving were identified for ships satisfying IMO intact stability criteria. Min et al. [13] also conduct free running model test for broaching. Wave excited yaw moment in following sea is measured using captive model experiments.

With the development of computational capabilities, time domain numerical simulation of surf-riding and broaching based on 4-DOF [14] and 6-DOF [15] models are conducted, and results are compared with experiments. A qualitative analysis is done by repeating numerical runs with many combinations of initial and control values to clarify critical conditions of motion [16]. However the numerical models used in the previous studies calculate the wave excitation force using the simplified Froude-Kriloff hypothesis on the mean water surface. Given that Froude-Kriloff force is critical for the occurrence of surf-riding at low frequency, it is of crucial importance to calculate Froude-Kriloff and restoring forces over the instantaneous ship wetted surface.

In this work, a 6-DOF weakly nonlinear model proposed by Yu, Ma and Gu [17] in which Froude-Kriloff and restoring forces are calculated nonlinearly are developed for the simulation of ship motions in following and quartering seas. The model couples the maneuvering and seakeeping motion based on the unified theory and incorporates rudder and propeller modeling. Each component of the model is verified based on the experiment data of the ITTC ship A2 provided in ref. [18]. Finally, results of numerical simulation are compared with the results of model experiments qualitatively.

2. Mathematical Model

2.1 Coordinate System

Three coordinate systems are used for describing ship motion, namely the earth fixed coordinate O_e-$x_e y_e z_e$, the body fixed coordinate O-xyz and the horizontal body axes coordinate O-$x_h y_h z_h$. The coordinate O-$x_h y_h z_h$ moves along with ship while its axes parallel to the axes of the Earth-fixed co-ordinate, as shown in Fig.1. The origin O is chosen at the ship center of gravity.

Ship forward speed is $\tilde{U}$. The position, velocity and force vectors are defined as:

$$\begin{aligned}\boldsymbol{\eta} &= \left[x, y, z, \phi, \theta, \psi\right]^T \\ \mathbf{v} &= \left[u, v, w, p, q, r\right]^T \\ \mathbf{f} &= \left[X, Y, Z, K, M, N\right]^T\end{aligned} \tag{1}$$

The velocity vector $\mathbf{v}$ which is defined in body-fixed coordinate will be transferred to earth-fixed coordinate:

$$\dot{\boldsymbol{\eta}} = \left[\dot{x}, \dot{y}, \dot{z}, \dot{\phi}, \dot{\theta}, \dot{\psi}\right]^T = \left[U, V, W, P, Q, R\right]^T = \begin{bmatrix} \mathbf{R}_{3\times3} & \mathbf{0}_{3\times3} \\ \mathbf{0}_{3\times3} & \mathbf{Q}_{3\times3} \end{bmatrix} \mathbf{v} \tag{2}$$

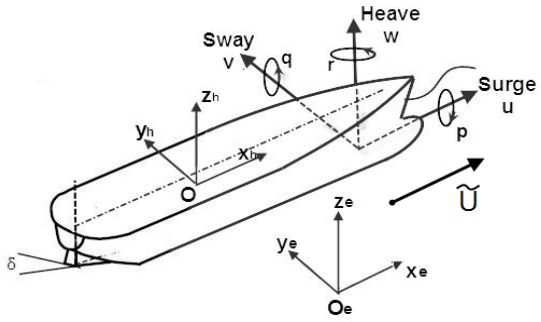

Fig. 1 Definition of coordinate system and ship motions

2.2 Maneuvering and Seakeeping Model

The maneuvering motion is simulated by a 3-DOF surge-sway-yaw MMG model, proposed by Japanese research group: Maneuvering Mathematical Modelling Group.

$$\begin{bmatrix} m-\bar{X}_{\dot{U}} & 0 & 0 \\ 0 & -m+\bar{Y}_{\dot{V}} & -mx_G+\bar{Y}_{\dot{R}} \\ 0 & -mx_G+\bar{N}_{\dot{V}} & -I_z+\bar{N}_{\dot{R}} \end{bmatrix} \begin{bmatrix} \dot{u} \\ \dot{v} \\ \dot{R} \end{bmatrix} + \begin{bmatrix} 0 & -mR & 0 \\ 0 & \bar{Y}_V & -mU+\bar{Y}_R \\ 0 & \bar{N}_V & -mx_G U+\bar{N}_R \end{bmatrix} \begin{bmatrix} u \\ v \\ R \end{bmatrix} = \begin{bmatrix} \bar{X}_{HO} \\ \bar{Y}_{HO} \\ \bar{N}_{HO} \end{bmatrix} + \begin{bmatrix} \bar{X}_\delta \\ \bar{Y}_\delta \\ \bar{N}_\delta \end{bmatrix} + \begin{bmatrix} -R(\tilde{U}) \\ +(1-t)T(\tilde{U}) \\ 0 \\ \\ 0 \end{bmatrix} \tag{3}$$

where *m* and *I* represent the ship mass and moment of

inertia, and(X_δ, Y_δ, N_δ), $R(\tilde{U})$ and $T(\tilde{U})$ are defined as rudder force, resistance and propeller thrust respectively. t is the propeller thrust deduction factor. (X_{HO}, Y_{HO}, N_{HO}) is higher order hull hydrodynamic force:

$$\begin{aligned}\bar{X}_{HO} &= X_{vv}v^2 + X_{vr}vr + X_{rr}r^2 \\ \bar{Y}_{HO} &= Y_{vvr}v^2r + Y_{vrr}vr^2 + Y_{vvv}v^3 + Y_{rrr}r^3 \\ \bar{N}_{HO} &= N_{vvr}v^2r + N_{vrr}vr^2 + N_{vvv}v^3 + N_{rrr}r^3\end{aligned} \tag{4}$$

The rudder forces are calculated:

$$\begin{aligned}\bar{X}_\delta &= -0.5(1-t_R)\rho A_R {U_R}^2 C_N \sin\alpha_R \sin\delta \\ \bar{Y}_\delta &= -0.5(1+a_H)\rho A_R {U_R}^2 C_N \sin\alpha_R \cos\delta \\ \bar{N}_\delta &= -0.5(GR_L + a_H x_H)\rho A_R {U_R}^2 C_N \sin\alpha_R \cos\delta \\ \bar{K}_\delta &= -GR\bar{Y}_\delta\end{aligned} \tag{5}$$

where K_δ is rudder moment on roll. A_R, U_R, GR, GR_L are the rudder area, the advance speed of rudder, the vertical and longitudinal distance between center of gravity and point of rudder force. And the rudder force coefficient C_N is determined empirically.

The sea-keeping motion is simulated by a 6-DOF model based on the IRF approach [19]. And the equation of motion can be written as:

$$\begin{aligned}&\sum_{j=1}^{6}\left[\left(m_{ij} + a_{ij}(\infty)\right)\dot{v}_j(t) + \int_0^t R_{ij}(t-\tau)v_j(\tau)d\tau + F_i^{res}(t)\right] \\ &= F_i^{FK}(t) + F_i^{dif}(t) + (\bar{K}_\delta, i=4)\end{aligned} \tag{6}$$

where m_{ij} and $a_{ij}(\infty)$ stand for the ship mass and the infinite-frequency added mass. And the nonlinear restoring forces, F-K forces and diffraction forces are denoted as $F_i^{res}(t), F_i^{FK}(t), F_i^{dif}(t)$. According to the IRF approach, the radiation and diffraction forces are calculated in frequency domain by the 2-D strip theory and transferred into time domain.

The restoring and Froude-Kriloff forces are calculated nonlinearly through pressure integration on instantaneous wetted surfaces. The hull and upper deck consist of several NURBS surfaces. Each surface has an area of A_i, a central point r_i=(x_i,y_i,z_i) with a normal vector n_i=(n_{xi},n_{yi},n_{zi}) in body-fixed axis. And the restoring forces and F-K forces are given as:

$$F_1^{FK\&res} = \sum_{i=1}^{N^*} A_i P(r_i^*, t) n_{xi}^* \tag{7}$$

$$P(r_i^*, t) = \rho g(d(x_i^*) - z_i^*) + A\rho g e^{k(z_i^* - d(x_i^*))}\cos(kx_i^* - \omega_e t)$$

$P(r_i,t)$ is the hydrodynamic pressure due to undisturbed waves. The superscript (*) indicates vectors in earth fixed coordinate system.

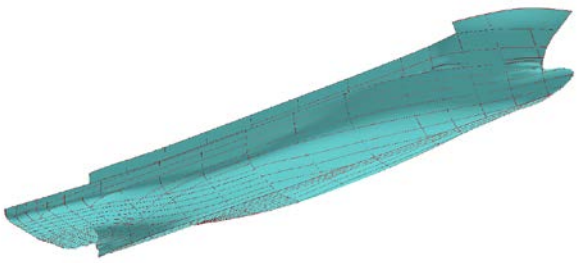

Fig.2 Hull NURBS sufaces of the ITTC ship A2

2.3 The Unified Model

In the unified model, the manoeuvring and seakeeping models described above are solved in different time scale. As a slowly varying motion, the manoeuvring motion is simulated using larger time step than the seakeeping motion. The seakeeping motion is simulated within each time step of the manoeuvring simulation assuming that the manoeuvring motion is constant. Then the total motion of the ship is calculated by combining the two motions referring to different coordinate system together:

$$\begin{aligned}&\left[X_T, Y_T, Z_T, \Phi_T, \Theta_T, \Psi_T\right] = \left[x^0, y^0, z^0, \phi^0, \theta^0, \psi^0\right] \\ &+\left[\int_0^t U_T dt, \int_0^t V_T dt, \int_0^t W_T dt, \int_0^t P_T dt, \int_0^t Q_T dt, \int_0^t R_T dt\right]\end{aligned} \tag{8}$$

where the subscript T indicates the total motion, and superscript 0 means the initial value for time t=0, and the seakeeping motion velocity in earth-fixed coordinate is given by:

$$[U_T, V_T, W_T, P_T, Q_T, R_T]^T = \begin{bmatrix}\mathbf{R}_{3\times3} & \mathbf{0}_{3\times3} \\ \mathbf{0}_{3\times3} & \mathbf{Q}_{3\times3}\end{bmatrix}[u_T, v_T, w_T, p_T, q_T, r_T]^T \tag{9}$$

Thus the sea-keeping and manoeuvring computations are coupled each other.

3. Model Verification

The model experiment data of the ITTC ship A2 provided in Ref. [18] are used for the verification of

the weakly nonlinear numerical model. Main particulars of the ship are shown in Tab. 1

Table 1 Main particulars of ITTC ship A2

	Ship	1/15 model
Length between per-pendiculars, Lpp(m)	34.5	2.3
Breadth, B(m)	7.60	0.507
Depth, D(m)	3.07	0.205
Fore draught, df(m)	2.5	0.166
Aft draught, da(m)	2.8	0.176
Mean draught, d(m)	2.65	0.186
Block coefficient, CB	0.597	0.597
Radius of gyration, roll, kxx/Lpp	0.108	0.108
Radius of gyration, pitch yaw, kyy/Lpp, kzz/Lpp	0.302	0.302
Longitudinal position of Buoyancy, LCB(m)	1.31m aft	0.087m aft
Longitudinal position of Floatation, LCF(m)	3.94m aft	0.263m aft
Metacentric height, GM(m)	1.00	0.0667
Natural roll period, TR (s)	7.4	1.9
	Bilge keel	model
Area, (m^2)	5.10 X2	0.023 X2
Position of fore end	6.22m fore	0.415m fore
Position of aft end	8.60m aft	0.573m aft
Breadth, (m)	0.35	0.023

All other data needed for the numerical simulation including hull geometry, hydrodynamic derivatives, rudder and propeller characteristics, roll viscous damping can be found in Ref. [18].

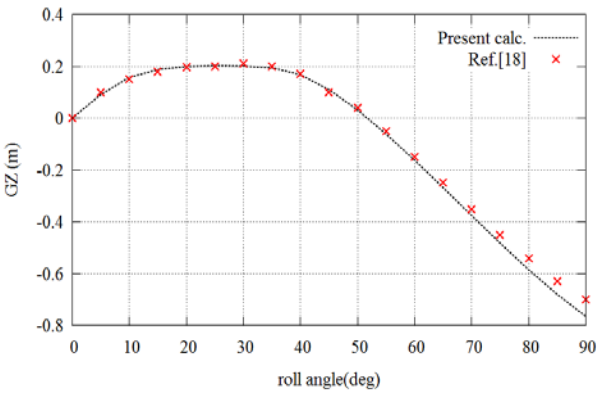

Fig.3 Comparison of GZ curve of Ship A2 in still water between present calculation and Ref.[18]

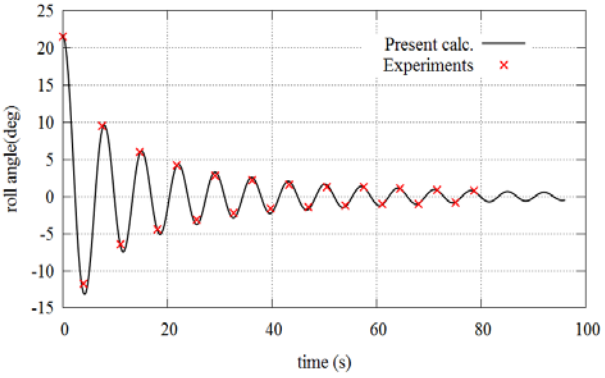

Fig.4 Comparison of roll decay test results between present calculation and experiments (Ref.[18])

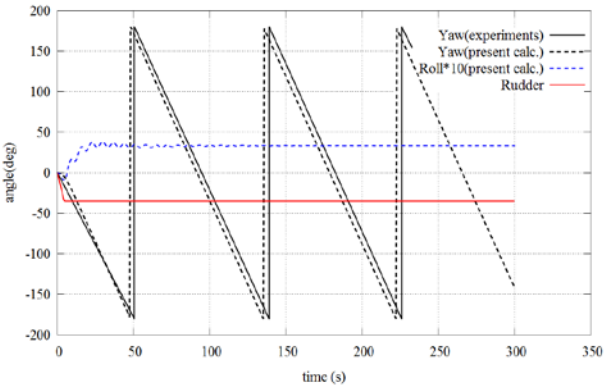

Fig.5 Comparison of -35 degree turning circle test results at Fn=0.30 between present calculation and experiments (Ref.[18])

GZ curve in still water is calculated using the code in which the pressure is integrated on instantaneous wetted surfaces and compared with the data provided in Ref. [18], and is shown in Fig.2. Roll decay test is also simulated to verify the seakeeping model. Results are compared with the roll decay experiment data and are shown in Fig.3. Moreover, the maneuvering model is verified by comparing with experiment results of the -35 degree turning circle test. However due to the lack of experiment data, only yaw angle in turning circle test is compared as shown in Fig.5. All the data is shown in full scale.

4. Numerical Simulation

According to Ref. [18], model experiments of ITTC ship A2 in quartering seas are conducted in various initial conditions with different ship speeds, wave lengths and autopilot courses. Periodic motion,

broaching, broaching without capsizing, nearly broaching and capsizing on a wave crest were identified from the experiment results. Four cases with full time series data are chosen for numerical simulation and they are shown in Tab.2.

Table 2 Cases for numerical simulation

No.	*Fn*	H/λ	λ/L_{pp}	χ	ω_e	Experiment results
1	0.3	1/8.7	1.127	-30	0.566	Periodic motion
2	0.3	1/10.0	1.637	-30	0.563	Periodic motion
3	0.43	1/8.7	1.127	-30	0.232	Capsize on a wave crest
4	0.431	0/10.0	1.637	-10	0.228	Capsize due to broaching

Where Fn is Froude number, H, λ, χ are wave height, length and heading angle, ω_e is encounter frequency. They satisfy the followings:

$$\omega^2 = gk(1+k^2H^2/4)$$
$$\lambda = 2\pi/k, \omega_e = \omega - kU\cos(\chi), U = \mathrm{Fn}\sqrt{gL_{pp}} \quad (9)$$

(1) Fn=0.3

For case No.1 and 2 with Froude number 0.3, numerical simulations are conducted with the same conditions as experiment. Results in full scale are demonstrated in Fig.6 and Fig.7.

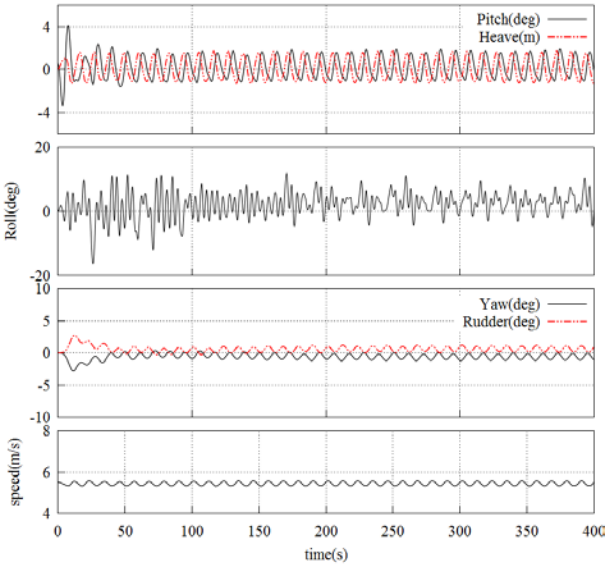

Fig.6 Result of case No. 1 in full scale with H/λ=1/8.7, λ/L_{pp}=1.127, *Fn*=0.3 and χ=-30 deg

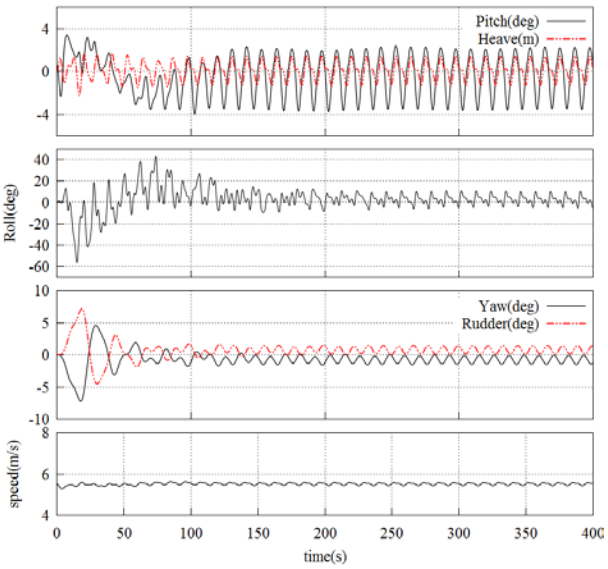

Fig.7 Result of case No. 2 in full scale with H/λ=1/10.0, λ/L_{pp}=1.637, *Fn*=0.3 and χ=-30 deg

As shown in Fig.6 and Fig.7, only periodic motion is observed for both cases with Froude number 0.3 and wave angle -30 degree, which is the same as experiment results.

(2) Fn=0.43

For case No.3 and 4 with Froude number 0.43, numerical simulations are conducted with the same conditions as experiment. Results in full scale are demonstrated in Fig.8 and Fig.9.

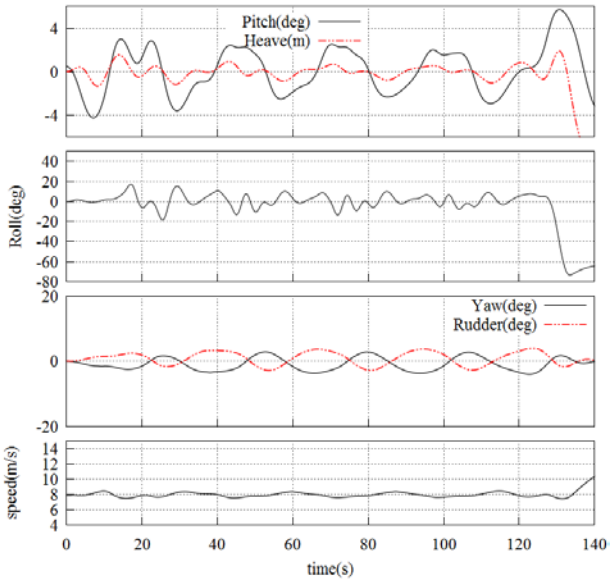

Fig.8 Result of case No. 3 in full scale with **H/λ=1/8.7**, λ/L_{pp}=1.127, *Fn*=0.43 and χ=-30 deg

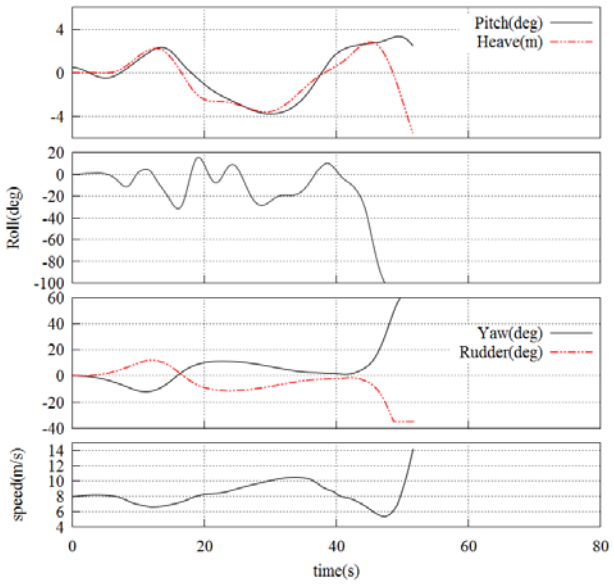

Fig.9 Result of case No. 4 in full scale with **H/λ=1/10.0**, λ/L_{pp}=1.637, *Fn*=0.43 and χ=-10 deg

From Fig.8, it is found that ship experiences very large heave and pitch motion after about 130s. This causes the reduction of restoring moment, and roll angle grows large consequently. Eventually ship capsizes due to loss of stability.

In Fig.9, the pitch angle keeps almost unchanged after 45s, and ship is sitting on the downslope of the wave. Meanwhile ship speed is accelerated to reach to wave celerity. This indicates that the ship is suffering surf-riding. At the same time, yaw angle increases suddenly and ship turns to port side, despite max rudder control is taken. Roll angle also starts to raise and eventually causes ship to capsize. Therefore, this implies that the phenomenon of capsizing due to broaching occurs, and broaching happens right after surf-riding.

Therefore, it has been shown that the weakly nonlinear model is capable of simulating ship stability failure events in quartering seas. However it should be noted that the actual wave heights used for numerical simulation in case No. 3 and 4 are H/λ=1/13.0 and 1/14.1, which is smaller than experiment. Because wave height higher than the value above will cause ship to capsize immediately. Thus the weakly nonlinear model tends to overestimate the possible stability failure events in following and quartering seas.

From results with different Froude number, it is found that ship tends to capsize at high Froude number in following and quartering seas. This is probably because that for high Froude number like Fn=0.43, the ship speed is close to wave celerity and ship may have encounter frequency close to zero. Hereby restoring and F-K forces are dominant; ship may be overtaken by wave from astern and experience stability loss. However for low Froude number like Fn=0.3, ship speed is much lower than wave celerity and it tends to do periodic motion. Therefore IMO Sub-Committee on Ship Design and Construction (SDC) suggests that a ship is considered not to be vulnerable to the broaching stability failure mode if Fn<0.3 [20].

5. Conclusions

In this work, a 6-DOF weakly nonlinear unified model considering nonlinear restoring and F-K forces over instantaneous wetted surfaces is applied for the numerical simulation of ship stability failure events in quartering seas. Due to the strong nonlinearity of broaching and surf-riding and lack of experimental data, the results are only compared with experiment results of the ITTC ship A2 qualitatively, but not quantitatively.

The weakly nonlinear model is proved to be capable of simulating ship stability failure events including broaching after surf-riding and capsizing due to loss of stability in quartering seas. However the weakly nonlinear model tends to overestimate the possibility of stability failure events in following and quartering seas.

It is also found that ship tends to capsize at high Froude number in following and quartering seas, due to the fact that ship may be overtaken by wave from astern with high speed close to wave celerity.

The weakly nonlinear model still needs to be improved and factors such as the reduction of rudder force, as well as the change of hydrodynamic derivatives and propeller characteristics in waves when surf-riding occurs should be investigated in

detail in the future.

References

[1] Mata-Álvarez-Santullano, F., Souto-Iglesias, A. (2014). Stability, safety and operability of small fishing vessels. Ocean Engineering, 79(0), 81–91.

[2] Grim, O. (1951). *Das Schiff in von achtern auflaufender See*. Schiffbau-Versuchsanstalt.

[3] Grim, O. (1963). Surging motion and broaching tendencies in a severe irregular sea. Deutsche Hydrografische Zeitschrift, 16(5), 201–231.

[4] Umeda, N., Kohyama, T. (1990). Surf-riding of a ship in regular seas. Journal of Kansai Society of Naval Architects.

[5] Umeda, N. (1999). Nonlinear dynamics of ship capsizing due to broaching in following and quartering seas. Journal of Marine Science and Technology, 4(1), 16–26.

[6] Makov, Y. (1969). Some results of theoretical analysis of surf-riding in following seas. T Krylov Soc, (126), 4.

[7] Maki, A., Umeda, N., Renilson, M., Ueta, T. (2014). Analytical methods to predict the surf-riding threshold and the wave-blocking threshold in astern seas. Journal of Marine Science and Technology, 1–10.

[8] Spyrou, K. J. (1995). Surf-riding and oscillations of a ship in quartering waves. Journal of Marine Science and Technology, 1(1), 24–36.

[9] Spyrou, K. J. (1996). Dynamic instability in quartering seas: The behavior of a ship during broaching. Journal of Ship Research, 40(1).

[10] Umeda, N., Hori, M., Hashimoto, H. (2007). Theoretical prediction of broaching in the light of local and global bifurcation analyses. International Shipbuilding Progress, 54(4), 269–281.

[11] Tigkas, I., Spyrou, K. J. (2012). Continuation Analysis of Surf-riding and Periodic Responses of a Ship in Steep Quartering Seas. In Proceedings of the 11th International Conference on the Stability of Ships and Ocean Vehicles (pp. 337–349).

[12] Umeda, N., Matsuda, A., Hamamoto, M., Suzuki, S. (1999). Stability assessment for intact ships in the light of model experiments. Journal of Marine Science and Technology, 4(2), 45–57.

[13] Min S. L., Ding Y., Zhao X. D. (1993). The tests on Broaching-to of a ship in following seas. Journal of Harbin Shipbuilding Engineering Institute, 14(3), 12–18.

[14] Umeda, N., Hamamoto, M. (2000). Capsize of ship models in following/quartering waves: physical experiments and nonlinear dynamics. Philosophical Transactions of the Royal Society of London. Series A: Mathematical, Physical and Engineering Sciences, 358(1771), 1883–1904.

[15] de Kat, J. O.,Pinkster, D.-J.,McTaggart, K. A. Random Waves and Capsize Probability Based on Large Amplitude Motion Analysis[J]. ASME Conference Proceedings, 2002, 2002 (36142): 685-694.

[16] Umeda, N., Hashimoto, H. (2002). Qualitative aspects of nonlinear ship motions in following and quartering seas with high forward velocity. Journal of Marine Science and Technology, 6(3), 111–121.

[17] Yu, L., Ma, N., Gu, X. (2012), “Study on Parametric Roll and Its Rudder Stabilization Based on Unified Seakeeping and Maneuvering Model”. 11th International conference on the Stability of Ships and Ocean Vehicles, Greece, 2012.

[18] Sample ship data sheet: ITTC A2 fishing vessel. Available online at http://www.naoe.eng.osaka-u.ac.jp/imo/a2

[19] Cummins, W.E., 1962. “The impulse response function and ship motions”, Schiffstechnik, 47(9), pp. 101-109.

[20] IMO SDC1/INF.8 ANNEX 15 (2014). Proposed Amendments to Part B of the 2008 IS CODE to Assess the Vulnerability of Ships to the Broaching Stability Failure Mode. London, UK: IMO SDC.